PHYSICAL REVIEW A, VOLUME 63, 043603

Multimode model of the formation of molecular Bose-Einstein condensates by Bose-stimulated Raman adiabatic passage

J. J. Hope, M. K. Olsen, and L. I. Plimak
Department of Physics, University of Auckland, Private Bag 92019, Auckland, New Zealand
(Received 5 July 2000; published 12 March 2001)

We investigate the conversion of a Bose-Einstein condensate (BEC) of a weakly interacting gas into a molecular BEC (MBEC) by Bose-stimulated Raman adiabatic passage (STIRAP). This method of producing an MBEC does not experience large spontaneous losses while the condensate is in an excited electronic state, and it is robust with respect to small changes in the physical parameters. We show that the atomic interactions affect the quantum statistics of the resulting field, although they do not interfere with the production of the MBEC. We demonstrate that STIRAP is still feasible when we include the spatial degrees of freedom that cause the Bose-enhanced coupling rate to vary across the condensate. The complete conversion is destroyed by spatial effects unless the time scale of the coupling is much faster than the propagation time, which in practice requires submillisecond conversion.

DOI: 10.1103/PhysRevA.63.043603 PACS number(s): 03.75.Fi, 32.80.Wr

I. INTRODUCTION

The Bose-Einstein condensation (BEC) of a weakly interacting atomic gas [1,2] has been of great theoretical and practical interest, and has recently led to the prediction of Bose-enhanced chemical processes, such as molecular photoassociation, at ultralow temperatures [3]. In a recent paper [4], Mackie *et al.* analyzed coherent two-color photoassociation of a Bose-Einstein condensate in the limit where the spatial structure and the nonlinearities due to the atomic interactions could be ignored. They showed that photoassociative Bose-stimulated Raman adiabatic passage (STIRAP) is a viable mechanism for converting an atomic condensate to a molecular condensate with near unit efficiency. We extend this model to include the spatial dependence of the atomic and molecular condensates, and include the effects of the interatomic interactions.

The process of STIRAP requires a pair of overlapping laser pulses, one of which couples the BEC from the atomic state to an excited molecular state, while the other couples the excited molecular field to a stable molecular state. These pulses are applied in the ''counterintuitive'' sequence, where the atomic field is first exposed to the laser that couples the two molecular states. Rather than attempting to combine the atoms within the BEC to produce molecules, this laser is defining the initial state of the BEC as a ''dark'' state, which does not interact with the laser. As the second pulse appears, the dark state becomes a linear combination of the two stable states. When the first pulse is finished, the stable molecular BEC (MBEC) is the equivalent dark state, as it is not affected by the laser that couples the atomic state to the excited molecular state. If the pulses are made sufficiently long, then the system adiabatically evolves from the stable atomic BEC to the stable molecular MBEC without producing a significant population in the excited MBEC.

STIRAP relies on the formation of the dark states and the ability to smoothly transfer from one to the other. Although the coupling strength of the atomic to molecular transition is quite weak [5], there is Bose enhancement of that transition rate, so its effective Rabi frequency can be made comparable to that of the excited-ground molecular transition, and Mackie *et al.* showed that this means that STIRAP may be a feasible method for producing an MBEC [4]. The model used in that paper ignored both the spatial structure of the condensates, and the effect of the interatomic interactions. The resulting model has formal similarities to traveling-wave second-harmonic generation [6], with the addition of an extra level. The atomic interactions will introduce a term analogous to a $\chi^{(3)}$ nonlinearity, which has been known to affect the quantum statistics in second-harmonic generation [7–10]. We therefore wish to examine the effects of the atomic interactions on the quantum statistics of the MBEC output.

A multicomponent BEC can only be described by a zero-dimensional model when each component can be described by a fixed spatial wave function. This requires the coupling to be spatially independent, and since the Bose enhancement (which we are relying on for the STIRAP to proceed) is density dependent, this condition is not met for this system. In real condensates, the interatomic interactions will cause further complications by making the spatial wave function of the trapped atoms depend on the total number of atoms in each component. For mean-field condensates, these effects can be modeled by the Gross-Pitaevski equation (GPE), which has already been used to describe Raman photoassociation in condensates by Heinzen *et al.* [3]. In that paper, a two-component mean field was coupled with a Raman transition that did not vary in time, and large oscillations between the two components were predicted.

In Sec. II, we will numerically solve the zero-dimensional model of STIRAP with the interactions included as a $\chi^{(3)}$ term, and examine the quantum-statistical features of the fields. In Sec. III, we extend the model to include the spatial degrees of freedom by using a nonlinear Schrödinger equation to describe the BEC and MBEC fields.

II. ZERO-DIMENSIONAL MODEL

Calculations of the quantum statistics of atomic fields can in principle be done by using phase-space techniques such as

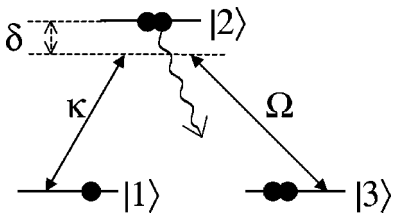

FIG. 1. Energy-level scheme for coherent free-bound-bound photoassociation. Levels $|1\rangle$, $|2\rangle$, and $|3\rangle$ are the electronic states for the atomic BEC, the excited MBEC, and the ground MBEC, respectively. $\tau(=\Omega_p t)$ is dimensionless.

the Wigner or positive-*P* representation [11,12]. In practice, these methods are considerably more difficult to apply to atomic fields than equivalent optical systems, as the interatomic interactions create nonlinear spatial effects that must be included in the calculations. This spatial dependence can only be ignored over very short time scales in which the kinetic-energy terms do not significantly couple the field between different locations. To gain a simple understanding of the quantum statistics of this system, we model each component of the BEC or MBEC as a single mode. This description will not be valid for time scales that are not much smaller than the time scale defined by the kinetic-energy term in the Hamiltonian. This is equivalent to considering the regime in which there is large coupling between the different components.

We are therefore describing the STIRAP process with three coupled modes, as in Mackie *et al.* [4]. The three modes are in a λ configuration as shown in Fig. 1, with state $|1\rangle$ being the atomic BEC, state $|2\rangle$ the excited state of the MBEC, and state $|3\rangle$ the stable MBEC. In a rotating frame, the interaction Hamiltonian may be written as

$$\frac{\hat{H}}{\hbar}=\delta\hat{b}^\dagger\hat{b}+i\kappa[\hat{a}^{\dagger 2}\hat{b}-\hat{a}^2\hat{b}^\dagger]+i\Omega[\hat{b}^\dagger\hat{c}-\hat{b}\hat{c}^\dagger]+\chi_a\hat{a}^{\dagger 2}\hat{a}^2+\chi_b\hat{b}^{\dagger 2}\hat{b}^2+\chi_c\hat{c}^{\dagger 2}\hat{c}^2, \tag{1}$$

where $\hat{a}$, $\hat{b}$, and $\hat{c}$ are the annihilation operators for $|1\rangle$, $|2\rangle$, and $|3\rangle$, respectively. The couplings for the $|1\rangle\leftrightarrow|2\rangle$ and $|2\rangle\leftrightarrow|3\rangle$ transitions have effective strengths κ and Ω, which are time dependent. We have ignored any interactions between the modes, as the magnitude of these interactions is not known. These interactions would be simple to include in the model, although if they were larger than the intracomponent interactions, they could lead to effects that would require the spatial structure to be included. In the high coupling limit, where the spatial structure can be ignored, the effect of all interactions will also be correspondingly reduced.

The Heisenberg equations of motion resulting from Eq. (1) are

$$\frac{d\hat{a}}{dt}=2\kappa\hat{a}^\dagger\hat{b}-2i\chi_a\hat{a}^\dagger\hat{a}^2, \tag{2a}$$

$$\frac{d\hat{b}}{dt}=-i\delta\hat{b}-\kappa\hat{a}^2+\Omega\hat{c}-2i\chi_b\hat{b}^\dagger\hat{b}^2, \tag{2b}$$

$$\frac{d\hat{c}}{dt}=-\Omega\hat{b}-2i\chi_c\hat{c}^\dagger\hat{c}^2, \tag{2c}$$

which as coupled nonlinear operator equations, have no known analytic solution. Hence, we proceed via the usual methods to derive *c*-number equations in the positive-*P* representation of quantum optics [13,14]. In order to write stochastic partial differential equations, we must use the positive-*P* for this system, as the *P* representation Fokker-Planck equation has a non-positive definite diffusion matrix and the Wigner representation gives derivatives of higher than second order [11,12]. In further calculations in this section, we will set $\chi_a=\chi_b=\chi_c=\chi$ and $\delta=0$. We find the following set of coupled Itô stochastic partial differential equations:

$$\begin{aligned}
\frac{d\alpha}{dt}&=-2i\chi\alpha^2\alpha^\dagger+2\kappa\alpha^\dagger\beta+\sqrt{2\kappa\beta-2i\chi\alpha^2}\,\eta_1(t),\\
\frac{d\alpha^\dagger}{dt}&=2i\chi\alpha^{\dagger 2}\alpha+2\kappa\alpha\beta^\dagger+\sqrt{2\kappa\beta^\dagger+2i\chi\alpha^{\dagger 2}}\,\eta_2(t),\\
\frac{d\beta}{dt}&=-2i\chi\beta^2\beta^\dagger-\kappa\alpha^2+\Omega\gamma+\sqrt{-2i\chi\beta^2}\,\eta_3(t),\\
\frac{d\beta^\dagger}{dt}&=2i\chi\beta^{\dagger 2}\beta-\kappa\alpha^{\dagger 2}+\Omega\gamma^\dagger+\sqrt{2i\chi\beta^{\dagger 2}}\,\eta_4(t),\\
\frac{d\gamma}{dt}&=-2i\chi\gamma^2\gamma^\dagger-\Omega\beta+\sqrt{-2i\chi\gamma^2}\,\eta_5(t),\\
\frac{d\gamma^\dagger}{dt}&=2i\chi\gamma^{\dagger 2}\gamma-\Omega\beta^\dagger+\sqrt{2i\chi\gamma^{\dagger 2}}\,\eta_6(t),
\end{aligned} \tag{3}$$

where there is a correspondence between $[\hat{a},\hat{a}^\dagger,\hat{b},\hat{b}^\dagger,\hat{c},\hat{c}^\dagger]$ and $[\alpha,\alpha^\dagger,\beta,\beta^\dagger,\gamma,\gamma^\dagger]$, although the latter are *c*-number variables that are not complex conjugate except in the mean of a large number of stochastic trajectories. This is due to the independence of the real noise terms, which have the properties $\overline{\eta_i(t)}=0$ and $\overline{\eta_i(t)\,\eta_j(t')}=\delta_{ij}\delta(t-t')$.

The model of Eq. (3) is similar to that used in Mackie *et al.* [4], except that we have included self-interactions via the $\chi^{(3)}$ nonlinearity and, by going to the positive-*P* representation, we have specifically included quantum effects. This model ignores the spatial structure of a real condensate, although it can be considered an approximation to a one-dimensional condensate in the limit where the kinetic-energy term in the Hamiltonian can be ignored. In the STIRAP case, as we show in Sec. III, this turns out to be a good approximation as long as the applied fields are of short duration.

To solve Eq. (3), we proceed via numerical stochastic integration, with the initial conditions that $\alpha(0)=\alpha^\dagger(0)=100$, the values for the other two fields being zero. These are all in coherent states, represented as δ functions in the *P*

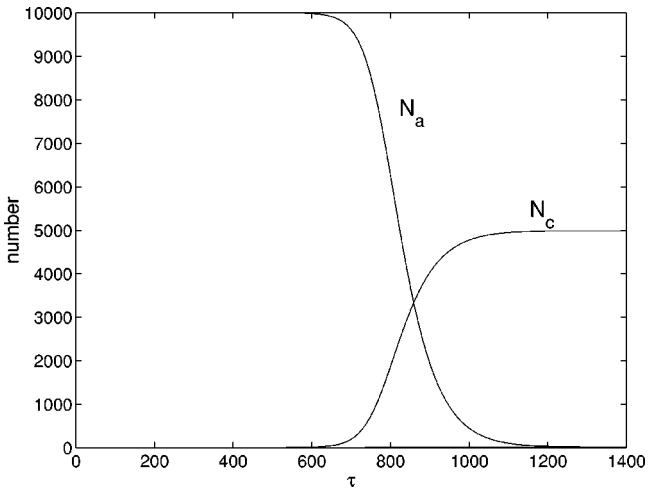

FIG. 2. The populations of N_a and N_c calculated using 10^5 stochastic trajectories. The maximum population of N_b is too small to appear at this scale. This figure does not noticeably change whether the $\chi^{(3)}$ interactions are included or not. $\tau(=\Omega_p t)$ is dimensionless.

representation. The true initial state is more likely to be sheared in a number-preserving way, producing a ''banana-shaped mode'' in the Wigner representation [15]. Such a state would be very difficult to write in the P representation without the use of generalized functions. However, the evolution of a coherent state will give a qualitative indication of the effects of the nonlinearities on the quantum statistics. The applied fields κ and Ω, are time-dependent Gaussian pulses:

$$\Omega(\tau)=\Omega_p \exp\left[-\frac{1}{2}\left(\frac{\tau-T_1}{\sigma}\right)^2\right],$$

$$\kappa(t)=\kappa_p \exp\left[-\frac{1}{2}\left(\frac{\tau-T_2}{\sigma}\right)^2\right], \tag{4}$$

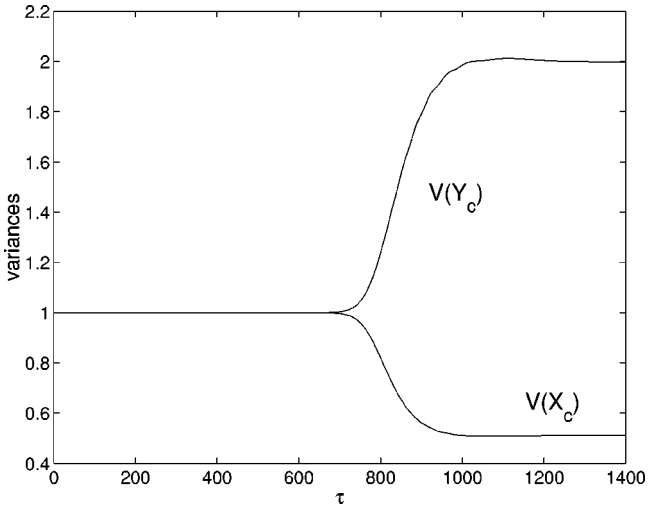

FIG. 3. The quadrature and number variances of the final state without the $\chi^{(3)}$ interaction. The final state is subPoissonian and squeezed in the amplitude quadrature. $\tau(=\Omega_p t)$ is dimensionless.

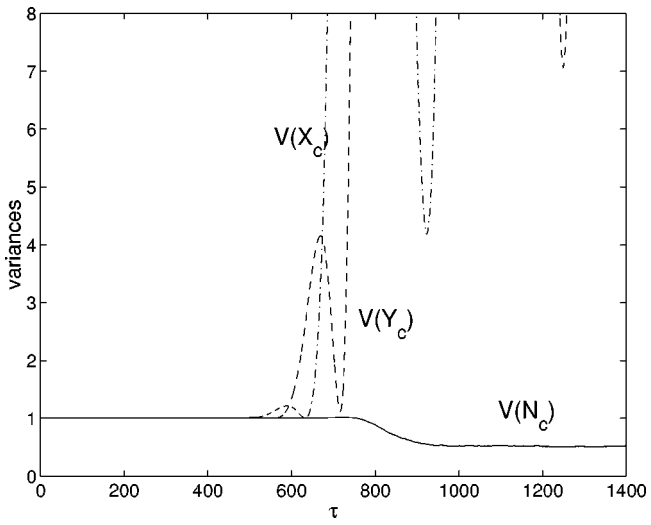

FIG. 4. The quadrature and number variances of the final state with the $\chi^{(3)}$ interaction included. The final state is subPoissonian, but there is no steady-state quadrature squeezing. $\tau(=\Omega_p t)$ is dimensionless.

where Ω_p and κ_p are the peak Rabi frequencies and we are using a dimensionless time $\tau=\Omega_p t$. The results shown in Fig. 2 were produced with the parameters $\kappa_p/\Omega_p=0.005$, $T_1=533$, $T_2=1025$, and $\sigma=133$, for which the stochastic integration was stable and there was a good conversion to the MBEC.

The quantities of interest are the numbers in each of the three states and the quantum statistics of the final state. As shown in Fig. 2, the mean number occupation of each mode does not change significantly with the addition of the self-interaction terms. We used a value $\chi/\Omega_p=10^{-4}$, which can be obtained by suitable choice of the coupling of the coupling strength Ω_p. For ''quick'' STIRAP, in which Ω_p is larger than 10 kHz, this value for χ is likely an overestimate.

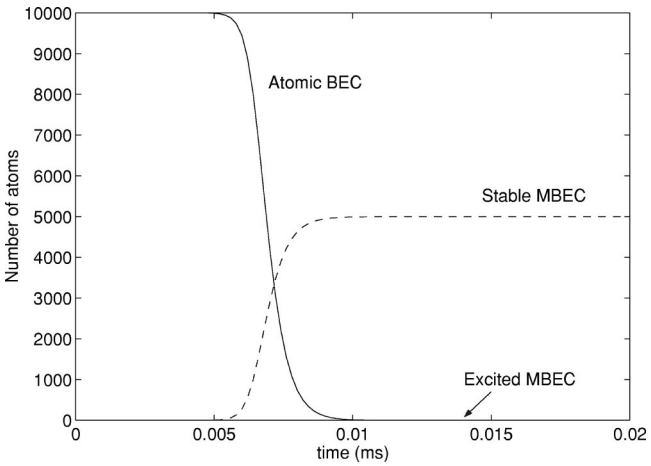

FIG. 5. The population transfer between the BEC and the MBEC. In this figure $T=2$ μs, $\Omega_p=200$ MHz, $\kappa_p=20$ kHz, and the atomic and trap parameters are as described in the text. All of the atoms have been converted to diatomic molecules, and the population of the excited MBEC is not visible on this scale.

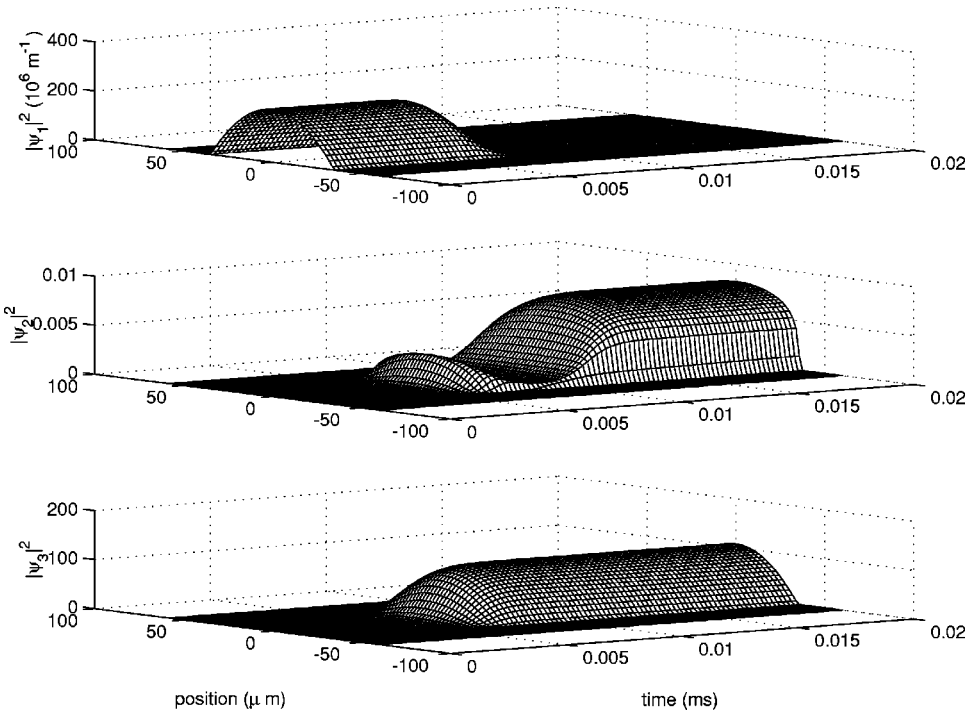

FIG. 6. The squared modulus of the wave functions as they develop in time. The upper plot shows the ground atomic state, the middle plot shows the intermediate state, and the lower plot shows the desired final molecular state. Note that the excited molecular state is essentially unpopulated.

We found that this actually decreased the maximum occupation of the intermediate dark state, from 9 (with $\chi=0$) to less than 1. On the scale of the figure, there is no visible difference in the dynamics whether or not $\chi^{(3)}$ is included.

Our primary interest in solving the zero-dimensional model is to determine the quantum statistics of the resultant field. To this end, we have calculated the quadrature variances for $X_c=c+c^\dagger$ and $Y_c=-i(c-c^\dagger)$, as well as the normalized intensity variance. A coherent state will have a quadrature and intensity variance of 1, a value of less than 1 for the quadrature variances represents squeezing, while a value of less than one for the intensity variance represents a subPoissonian field. Without the self-interactions, we find that the resultant field is a little less than 50% squeezed in the X_c quadrature, as shown in Fig. 3. The field is still close to being in a minimum uncertainty state and has a normalized intensity variance indistinguishable from the variance in X_c. This is typical of resonant $\chi^{(2)}$ interactions where the mean fields remain real, as the Wigner function ellipse is squeezed, but neither rotated nor moved off the X axis.

The 50% amplitude squeezing in the MBEC is a direct consequence of the fact that the process is completely converting a coherent BEC to diatomic molecules, which in the number basis simply compresses the scale of the number distribution by a factor of 2.

When we add the nonzero $\chi^{(3)}$ component, we find a significant difference in the quantum state of the output mode, although the dynamics are essentially unchanged. As seen in Fig. 4, while the normalized intensity variance is almost unchanged, there is now no squeezing in either quadrature. Examination of the variances at different quadrature angles shows that the minimum quadrature noise continues to increase while the intensity noise stays constant. This is a signature of $\chi^{(3)}$ systems and indicates that there is a rotation and deformation of the Wigner ellipse of the initial coherent state. This effect has previously been calculated for the condensate [15], showing that the contours of the Wigner function take on a bananalike shape, which would indeed give subPoissonian statistics at the same time as excess quadrature noise.

III. MODEL IN ONE DIMENSION

We have shown that the interactions do not adversely affect the population transfer to the MBEC, but we have ignored any possible spatial effects. In this section, we describe these effects with a mean-field model.

When the kinetic energy can be ignored, the fields at dif-

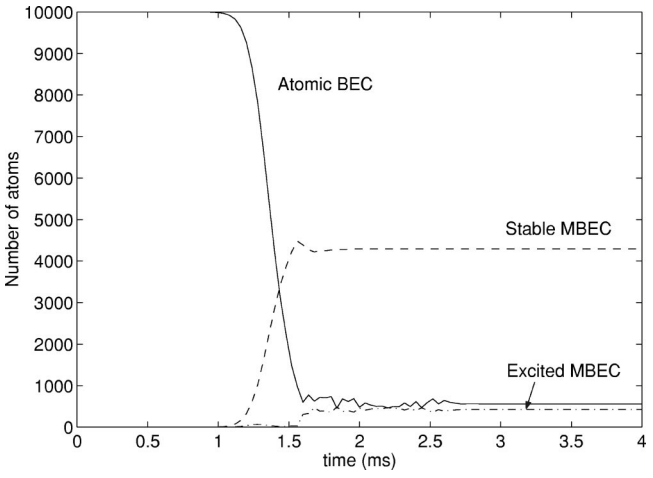

FIG. 7. The population transfer between the BEC and the MBEC. In this figure $T=0.4$ ms, $\Omega_p=1$ MHz, $\kappa_p=100$ Hz, and the atomic and trap parameters were as described in the text. For this longer time scale, the population of the excited state MBEC is quite significant.

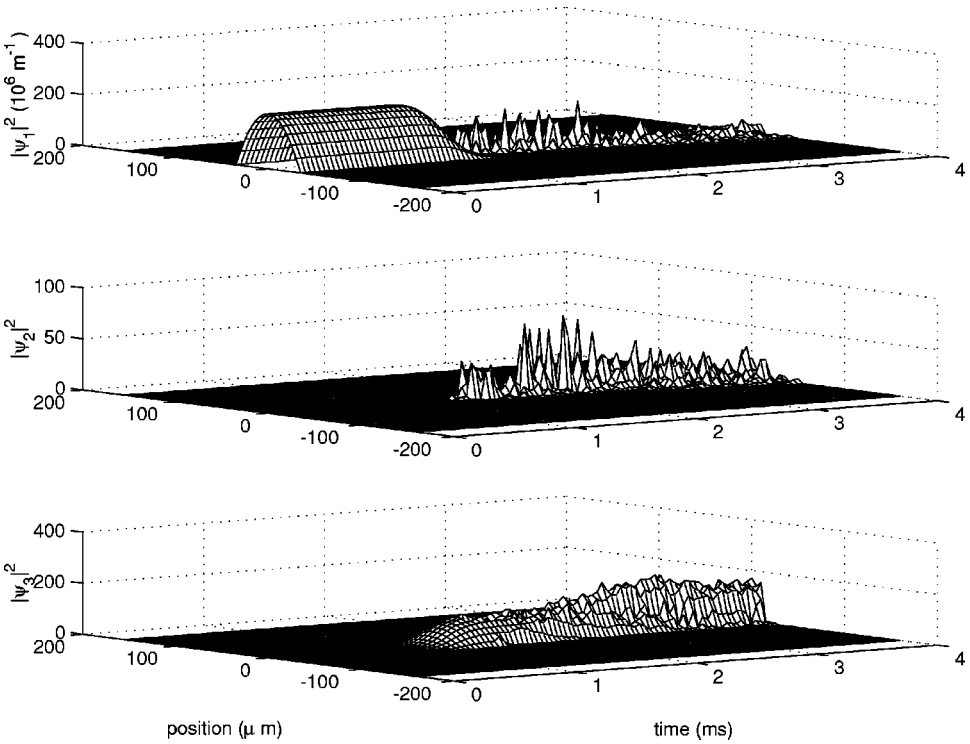

FIG. 8. The squared modulus of the wave functions as they develop in time. The upper plot shows the ground atomic state, the middle plot shows the intermediate state, and the lower plot shows the desired final molecular state. Note that the excited molecular state is essentially unpopulated.

ferent points in space are not coupled, and the fields decouple into a set of three component zero-dimensional systems as described in Sec. II. Each subsystem is described by the three components at a single point. We have shown that it is possible to choose coupling parameters for this system that produce an MBEC without producing excited molecules. This transfer is most reliable when the Bose enhancement of the free-bound transition is sufficiently large to be comparable to the bound-bound Rabi frequency. The process of STIRAP requires the effective ratio of the two Rabi frequencies to start off close to zero and slowly change to become extremely large. This condition is most easily satisfied when the peak values are comparable. Any asymmetry will make one condition stronger, but make the other one weaker. As the Bose enhancement is proportional to the square root of the density of the field, we can see that it is only possible to have the effective peak Rabi frequencies equal at a single point in space. For higher densities, the free-bound transition will peak stronger than the bound-bound transition, and for lower densities it will be weaker.

The presence of the kinetic-energy term couples the fields at different points in space, and since they are proceeding through the transition from one dark state to the other at different rates, this could possibly destroy the ''darkness'' of the dark states. Fortunately, the requirement that the laser pulses be changed adiabatically only means that they have to be changed slowly on the time scale of the inverse Rabi frequency. This means that the high laser power can make the adiabatic transition very quickly. This allows us to produce the MBEC over a time scale that is much shorter than that of the nonlocal coupling produced by the kinetic energy.

We describe each electronic state of the BEC as a mean field that evolves by the one-dimensional GPE. This includes the spatial dependence of the field and can include the effects of the interatomic interactions. The lasers coupling the BEC and MBEC components are assumed to be spatially much broader than the condensates, so the coupling coefficients do not depend on position.

The resulting equations of motion are

$$
\begin{aligned}
i\hbar\frac{\partial}{\partial t}\psi_1(x) &= \left(-\frac{\hbar^2}{2M}\nabla^2 + V_1(x) + U|\psi_1(x)|^2\right)\psi_1(x) \\
&\quad - 2\hbar\kappa(t)\psi_1^\dagger(x)\psi_2(x), \\
i\hbar\frac{\partial}{\partial t}\psi_2(x) &= \left(\hbar\delta - \frac{\hbar^2}{2M}\nabla^2 + V_2(x) + U|\psi_2(x)|^2\right)\psi_2(x) \\
&\quad - \hbar\kappa(t)\psi_1(x)^2 - \hbar\Omega(t)\psi_3(x), \\
i\hbar\frac{\partial}{\partial t}\psi_3(x) &= \left(-\frac{\hbar^2}{2M}\nabla^2 + V_3(x) + U|\psi_3(x)|^2\right)\psi_3(x) \\
&\quad - \hbar\Omega(t)\psi_2(x),
\end{aligned}
\tag{5}
$$

where ψ_1 is the mean field of the atomic BEC, ψ_2 and ψ_3 are the mean fields for the excited and ground MBEC, respectively, V_j is the trap potential for corresponding field ψ_j, $\kappa(t)$ is the Rabi frequency for the free-bound photoassociation, and $\Omega(t)$ is the Rabi frequency for the excited-stable molecular transition. The mean fields are normalized to the total atom number, so $\int dx[|\psi_1(x)|^2 + 2(|\psi_2(x)|^2 + |\psi_3(x)|^2)] = N$, where N is the total number of atoms, including those in the molecules.

We solve these equations numerically, beginning with an atomic BEC in the ground state. We use a split-step operator method implemented by a package called XMDS, which solves nonlinear PDEs [16]. Our simulations show that with

κ chosen to make the coupling rate symmetric at half of the peak density, we have an almost complete transfer from the stable atomic BEC to the molecular MBEC. The population of the excited-state MBEC is of a similar order to the residual population in the atomic BEC, and both are negligibly small. This transfer is shown in Figs. 5 and 6. We used typical atomic and trap parameters: $M=5\times10^{-26}$ kg and $V(x)=M\omega^2x^2/2$, where $\omega=773$ Hz.

Both laser pulse shapes were Gaussian [4]:

$$\omega(t)=\Omega_p \exp(-(t-2.5T)^2/T^2),$$
$$\kappa(t)=\kappa_p \exp[-(t-4.5T)^2/T^2], \tag{6}$$

where T is the length scale of the pulses, and for the adiabatic condition to hold $\Omega_pT\gg1$. The value for κ_p is chosen so that $\kappa_p\psi_1(x,0)\approx\Omega_p$ for the largest possible number of atoms.

The results in Figs. 5 and 6 are obtained using powerful pulses that are only a few microseconds long. When the pulses are applied for longer times, the kinetic energy couples the field between different positions and disturbs the dark states. This means that significant populations of excited molecules can be produced. In this situation, the spatial structure becomes more complicated, as there is a large amount of energy bound up in the mean-field interactions that is being partially converted to kinetic energy.

Figure 7 shows the population transfer that occurs when the STIRAP process takes place over several milliseconds. The figure of merit for the adiabaticity Ω_pT is the same, and in the absence of kinetic energy this figure would look identical to Fig. 5. When we include the spatial structure, we find a large population in the molecular excited state.

When the interaction takes place more slowly, the spatial structure of the condensate gets significantly disturbed. The interactions are so large in these systems that the kinetic energy barely affects the shape of the ground state, so it is not surprising that condensates are very sensitive to disturbances. For the same reasons, the GPE becomes quite stiff in these parameter regimes, so it becomes a lot more difficult to make detailed calculations. The parameters used in Fig. 7 are taken from the onset of this stiff regime, and the mean field is already looking complicated. The density function of each condensate is shown in Fig. 8.

IV. CONCLUSIONS

We have shown that the transfer of atoms to molecules via STIRAP is robust with respect to detunings, $\chi^{(3)}$ nonlinearities, and small asymmetries between the peak strengths of the two Raman lasers. This enables the process to provide a complete population transfer by two short, powerful, overlapping laser pulses. The complete conversion is destroyed by spatial effects unless the time scale of the coupling is much faster than the propagation time. For the parameters used in this paper, this meant that the entire conversion process had to take place on a submillisecond time scale. The output MBEC is likely to exhibit some interesting quantum statistical features, including suppression of noise in the particle number due to the atomic combination.

ACKNOWLEDGMENTS

This research was supported by the University of Auckland Research Committee and the Marsden Fund of the Royal Society of New Zealand.

[1] M. H. Anderson *et al.*, Science **269**, 198 (1995).
[2] A. S. Parkins and D. F. Walls, Phys. Rep. **303**, 1 (1998).
[3] D. J. Heinzen, R. Wynar, P. D. Drummond, and K. V. Kheruntsyan, Phys. Rev. Lett. **84**, 5029 (2000).
[4] M. Mackie, R. Kowalski, and J. Javanainen, Phys. Rev. Lett. **84**, 3803 (2000).
[5] J. Javanainen and M. Mackie, Phys. Rev. A **58**, R789 (1998).
[6] M. K. Olsen, R. J. Horowicz, L. I. Plimak, N. Treps, and C. Fabre, Phys. Rev. A **61**, 021803(R) (2000).
[7] M. K. Olsen, V. I. Kruglov, and M. J. Collett (unpublished).
[8] C. Cabrillo and F. J. Bermejo, Phys. Lett. A **170**, 300 (1992).
[9] K. V. Kheruntsyan, D. S. Krähmer, G. Yu. Kryuchkyan, and K. G. Petrossian, Opt. Commun. **139**, 157 (1997).
[10] C. Cabrillo, J. L. Roldán, and P. García-Fernandez, Phys. Rev. A **56**, 5131 (1997).
[11] M. J. Steel *et al.*, Phys. Rev. A **58**, 4824 (1998).
[12] P. D. Drummond and J. F. Corney, Phys. Rev. A **60**, R2661 (1999).
[13] P. D. Drummond and C. W. Gardiner, J. Phys. A **13**, 2353 (1980).
[14] C. W. Gardiner, *Quantum Noise* (Springer-Verlag, Berlin, 1991).
[15] J. A. Dunningham, M. J. Collett, and D. F. Walls, Phys. Lett. A **245**, 49 (1998).
[16] G. R. Collecut, P. D. Drummond, and H. He, http://www.physics.uq.edu.au/xmds/